Meteorol. Appl. 6, 261–271 (1999)

Influence of weather conditions on the distribution of persistent contrails

Martina Kästner, Richard Meyer and Peter Wendling, *DLR Oberpfaffenhofen, Institut für Physik der Atmosphäre, Post-box 1116, D-82230 Wessling, Germany*

An automated contrail detection algorithm has been applied to AVHRR data to obtain the position of contrails. Nearly simultaneous data from the Europe Model of the Deutscher Wetterdienst have been used to find typical weather conditions associated with 742 persistent contrails. Further, a flow pattern analysis identifies typical regions where the occurrence of contrails was above average. These regions are in the upper atmosphere: (a) ahead of a surface warm front either in moist warm layers before the cirrus clouds arrive or more likely with the cirrus in a warm conveyor belt and (b) ahead of a surface cold front in rapidly moving cold air in the turbulent regions near a band of strong wind (though the speed is not necessarily as high as in a jet). Usually, the atmosphere is baroclinic in the contrail region. Most of the detected contrails occur in divergent flow patterns in the upper troposphere in slowly rising warm or locally turbulent cold air masses.

1. Introduction

Contrails are generated by aircraft emissions below a certain cold threshold temperature which depends on engine specific parameters (Appleman, 1953; Schumann, 1996). The artificial clouds form from droplets of condensed water vapour which freeze at once, forming ice crystals. These grow at the expense of supercooled water droplets and of the water vapour of the ambient atmosphere or they sublimate. The total number of ice crystals produced is similar to the number of droplets expected in the initial liquid water contrail (Knollenberg, 1972). Long-living contrails indicate moist layers in the upper troposphere where there is either rapidly moving cold air or slowly ascending warm air. A relationship between the spreading of a contrail and the wind speed at upper-tropospheric levels has already been identified by Peppler (1930). This relationship was further confirmed by the investigation of Travis (1996) which is based on the use of satellite and radiosonde data for a large number of contrails. Specifically, contrail widths are positively correlated with the 300–100 hPa wind shear and the average wind speed of this layer. The increase in contrail width is due to the increase in turbulence in strong wind situations leading to an enhancement of the rate of entrainment of moisture from the ambient air.

Recently, many measurements from the ground, aircraft and satellites have remarkably increased the physical understanding of contrails. Information about the extent and growth of contrails is given in Freudenthaler *et al.* (1995) and Spinhirne *et al.* (1998), and the chemical situation in and around contrails is described by Kaercher *et al.* (1996). Visual inspection of NOAA–AVHRR images gave a typical cloud cover of contrails of about 1% over Europe and a typical annual cycle with a maximum in summer and a minimum in autumn (Bakan *et al.*, 1994). Contrails moderate the radiative transfer within the atmosphere (Liou, 1986) and those in clear sky conditions have the greatest potential to modify the radiation balance. The radiative impact of an increase of 1% by artificial cloud cover is estimated to be about 0.1 K (Strauss *et al.*, 1997). Therefore, the climatic affect of contrails could be important if the flight traffic increases considerably in the next decade and this results in an increase in cloud cover due to contrails along the traffic routes (Ponater *et al.*, 1996; Sausen *et al.*, 1998).

Unknown until now is when, where and how often contrails occur; a contrail climatology is missing. In this study typical properties of the atmosphere (based on model fields) when contrails occur are examined in a test area of 6° longitude by 4° latitude in central Europe. With these properties the contrail regions could be identified and, with an assumed flight traffic increase, GCM simulations could be used to give a prediction of the global impact of contrails.

The aim of this study is to determine the atmospheric conditions that support persistent contrails; this is unlike previous studies, which have focused on the microphysical conditions behind an aeroplane. Satellite observations show that there are regions with contrails and neighbouring regions with none. What is the difference between these regions? The air traffic in central Europe is dense enough to fulfil the assumption that contrails occur in any region where long-living contrails are possible. In this study the frequency of con-

trail occurrence rather than the contrail cloud cover is determined as a function of cyclonic or anticyclonic flow pattern from various directions.

The source of data and their quality, and the method used, are described in section 2. The frequency and geographical distribution of contrails are given in section 3, their thermodynamic parameters are reported in section 4, and the results of the analysis of weather conditions are given in section 5 and discussed in section 6.

2. Data and method

Extensive contrail regions can often last for several hours (Travis *et al.*, 1997). Those regions where contrails frequently occur are analysed in this study. An automated algorithm was applied to NOAA–AVHRR measurements (Mannstein *et al.*, 1998) to determine the position of linear contrails – only these form the basis of this study. This pattern recognition scheme searches for contrails in the temperature difference image of channels 4 and 5, a procedure suggested by Engelstad *et al.* (1992), and in the temperature image of channel 4. If a line filter is applied in various directions to both images, contrail-like structures are preselected and then classified by additional geometrical and physical criteria.

As a first step, the thermodynamic parameters at the nearest grid point of the Europe Model (EM) of the Deutscher Wetterdienst (DWD) were inspected to identify typical properties when contrails occur. A similar procedure was carried out for neighbouring regions where no contrails were evident. Most of the contrails accompany natural cloud systems. Both data sets (with and without contrails) are examined for significantly different properties. The selected thermodynamic parameters are specific humidity and temperature (i.e. implicitly the relative humidity over ice (Sonntag, 1994)), the horizontal wind components u and v, and the vertical motion ω. The altitude is known from the geopotential.

The EM is a hydrostatic meso-α scale regional numerical weather prediction model for the North Atlantic and Europe. The prognostic variables are surface pressure, total heat, total water content and horizontal wind components; its diagnostic variables are temperature, water vapour and cloud water contents, geopotential and vertical velocity. The numerics are operated on a mesh size of about 55 km, in 20 hybrid layers, and the time integration is made in a 5-minute step. The boundary values are provided by the Global Model at three-hourly intervals.

The study was carried out for January and April in 1996 and 1997. Daily one NOAA–AVHRR overpass was used, which was asynoptic but always at about midday. Further, hourly EM predictions were used; these have high quality at prediction times 00+11 to 00+13 UTC. The time difference between model and AVHRR data was always less than 30 minutes.

The AVHRR nadir resolution is 1.1 km. Many contrails are smaller in width but they were usually detectable because a contrast with the neighbouring pixel was already reached through subpixel structures. The contrail detection was highly efficient in regions with a small temperature variance (e.g. over water or fog).

The second approach relied on the analysis of the wind direction taken from the EM data and the cyclonic or anticyclonic curvature of the flow. In cases of ambiguity the curvature is determined from a 500 hPa map at 1200 UTC, because this map was available in a much better scale than the more appropriate 300 hPa map. As the test area is small, being only 440 km × 450 km (Figure 1), the flow could be categorised by one upper wind direction and whether the curvature is cyclonic or anticyclonic. Further, the air masses could be classified according to their origin; they have quasi-homogeneous properties in temperature, humidity, and stability profiles. The operational DWD classification of so-called 'Großwetterlage' (Gerstengarbe & Werner, 1993) is used.

The test area in central Europe is shown in Figure 1 (9°–15° E, 47°–51° N) and hereafter simply referred to as Bavaria. Figure 2 shows the EM grid points, which are 55 km apart. It is assumed that in each EM cell the thermodynamic parameters are homogeneous. Figure 3 shows the contrails detected on 14 January 1996 in Bavaria with a 1° grid overlaid; it is a day with many contrails. The contrail detection algorithm utilises both the difference of brightness temperatures of AVHRR

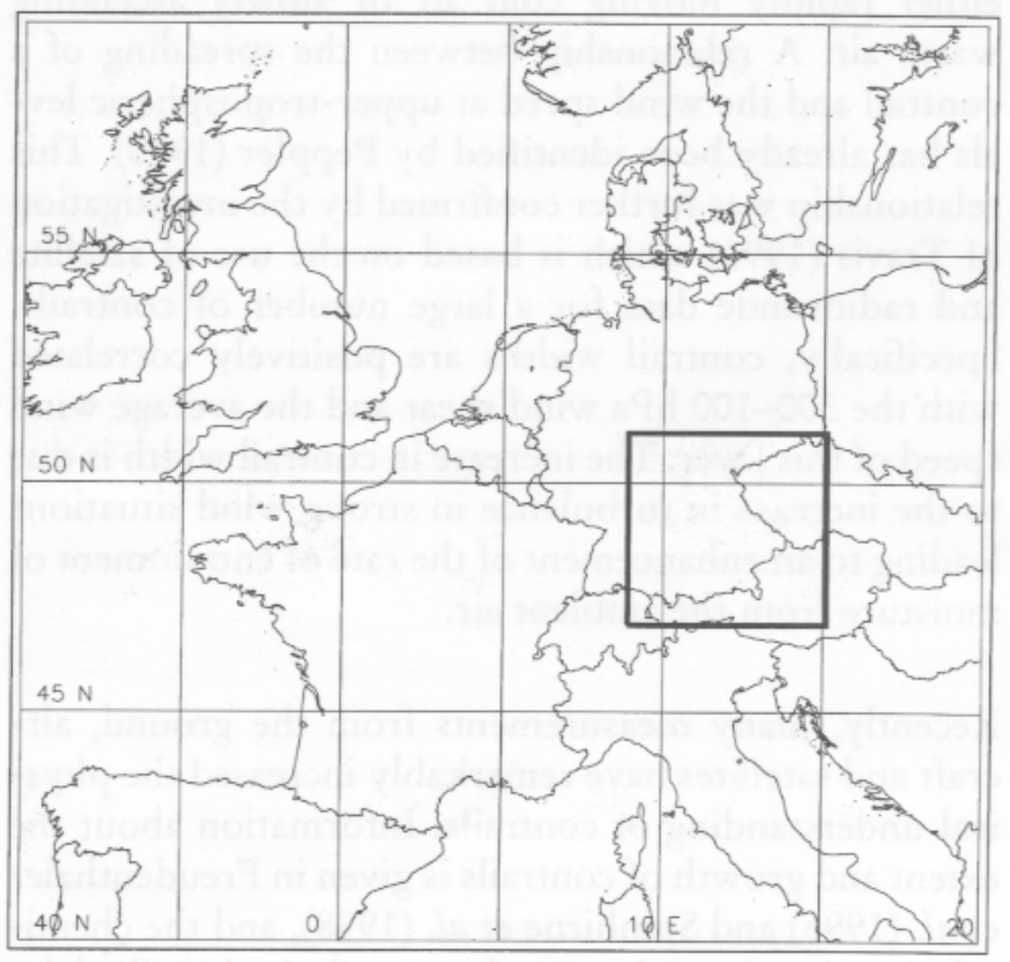

Figure 1. *Test area in central Europe.*

channels 4 and 5 (Figure 4) and the brightness temperature of channel 4 (Figure 5).

For 742 contrails from a total of 122 days the grid point values are read from the overlaid pixelwise contrail mask into a data set called 'with contrails' and another 'without contrails'. Whenever a contrail crosses a box it is added to the data set 'with contrails'.

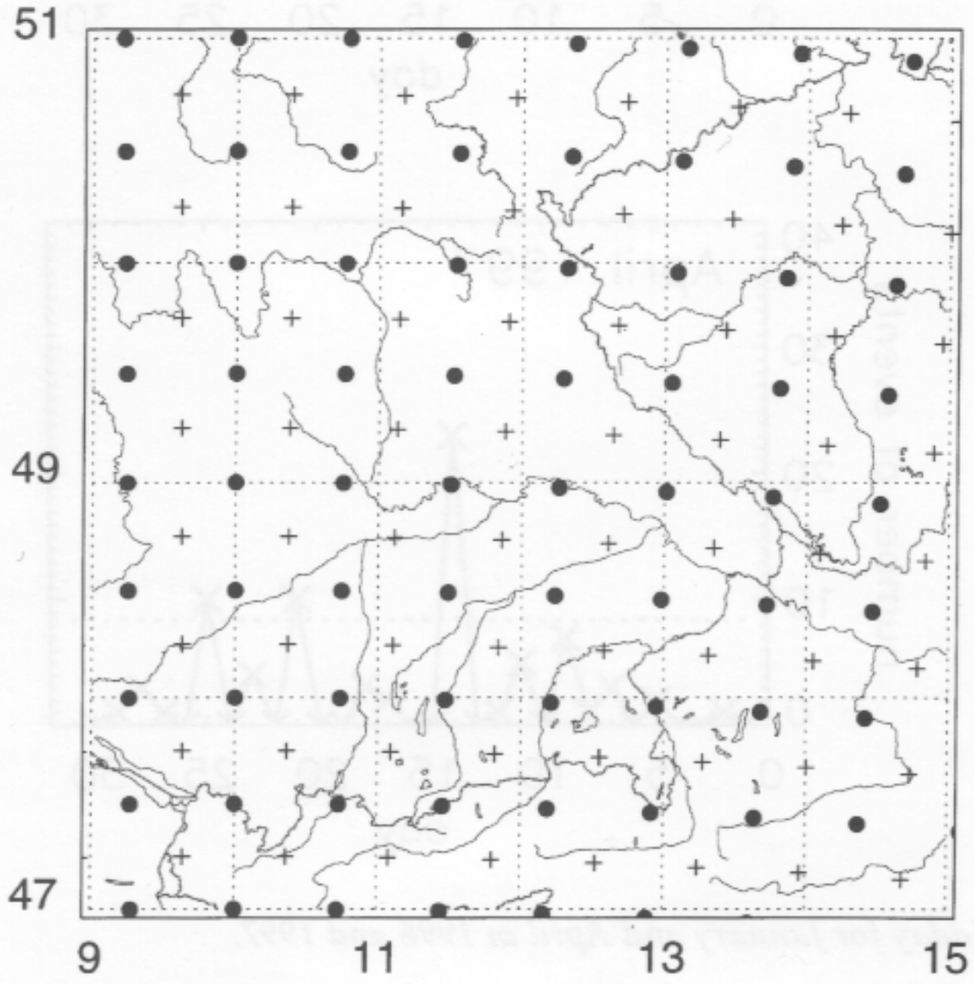

Figure 2. *EM grid points (dots) in the test area. Each grid point is surrounded by crosses indicating an EM cell, which is assumed to have homogeneous thermodynamic parameters inside. A 1° grid, national boundaries and rivers are drawn for better orientation.*

3. Frequency and distribution of contrails

The number of contrails detected in AVHRR images at midday is shown for each day of the four months in Figure 6. Also shown is the mean contrail intensity given by the number of contrails (742) per contrail day (88 days); the mean contrail intensity depends on the extent of the test area. Figure 6 shows that the mean

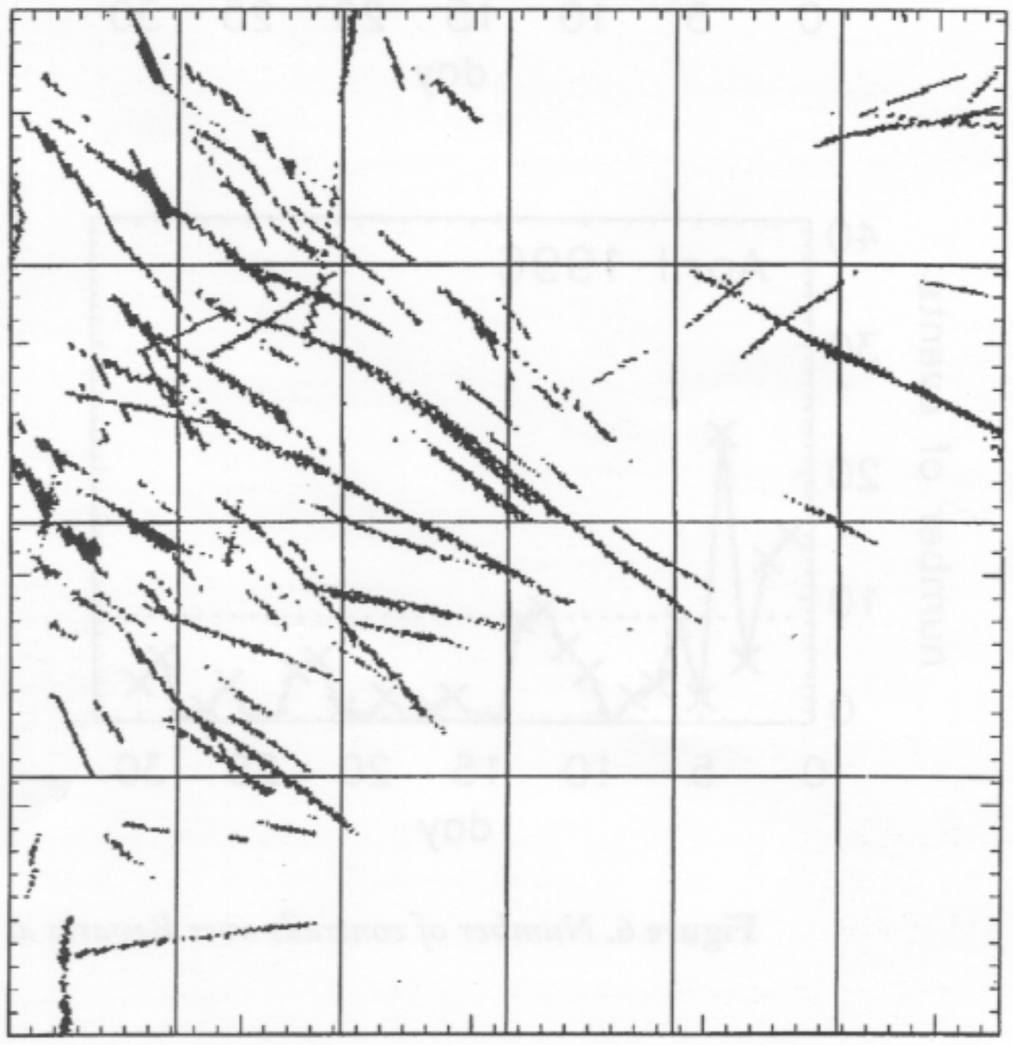

Figure 3. *Contrails detected by the pattern recognition scheme after Mannstein et al. (1998) applied to AVHRR data from 14 January 1996, 1143 UTC.*

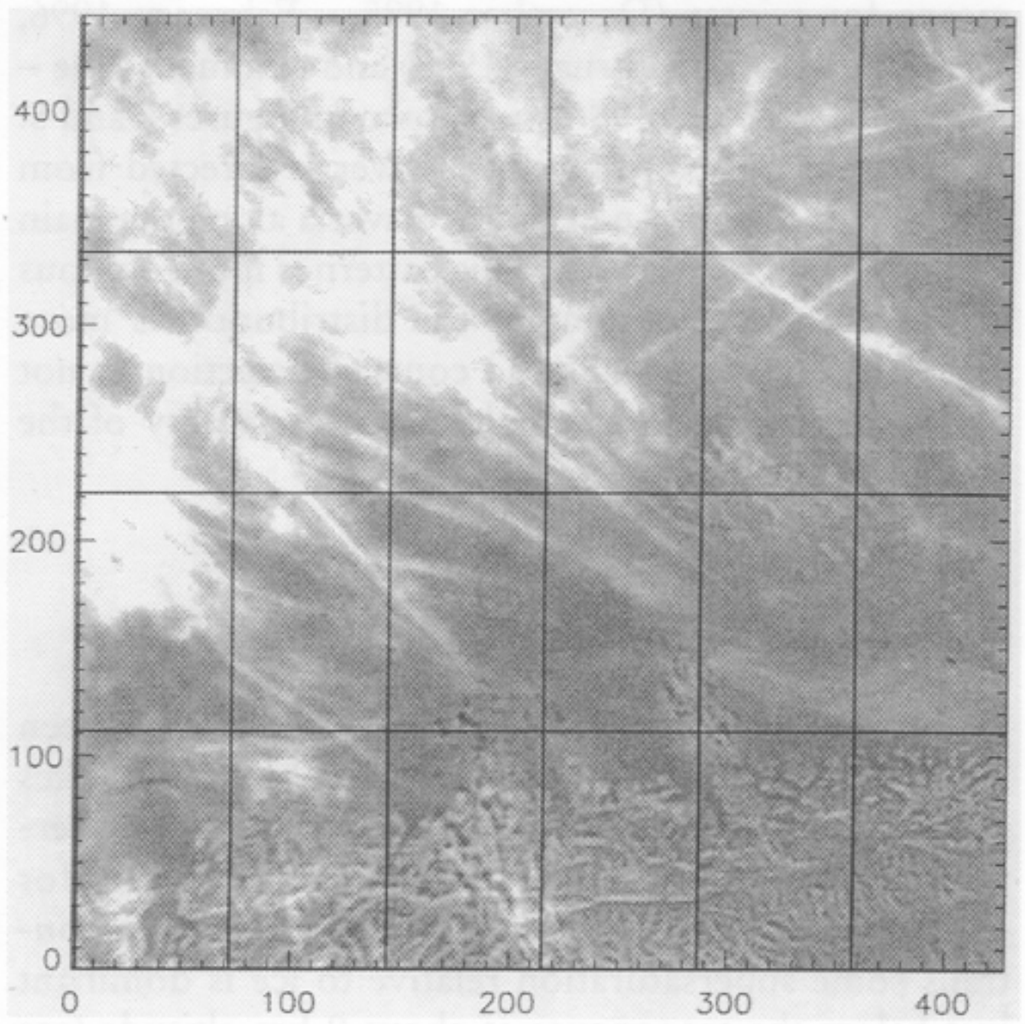

Figure 4. *Radiance difference of AVHRR channels 4 and 5 (T4–T5) for the same scene as in Figure 3.*

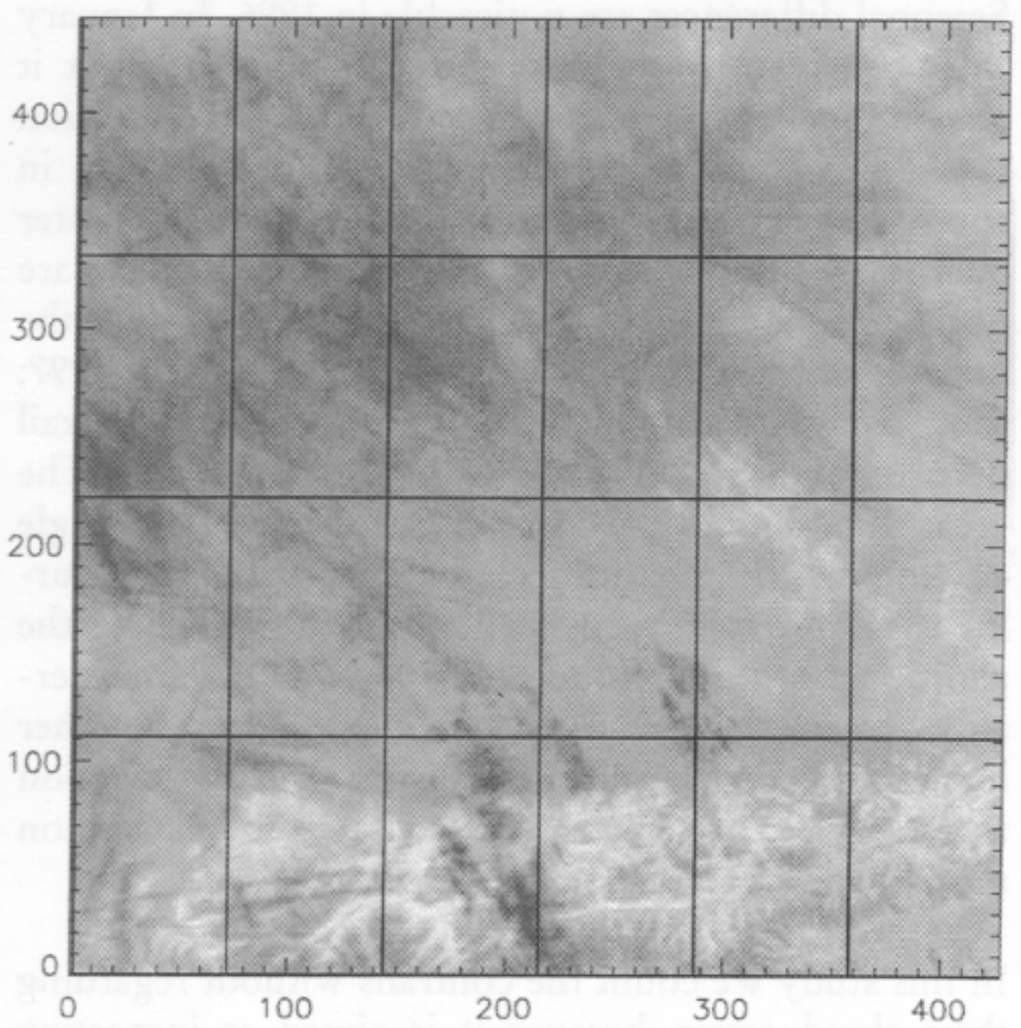

Figure 5. *Radiance of AVHRR channel 4 (T4) for the same scene as in Figure 3.*

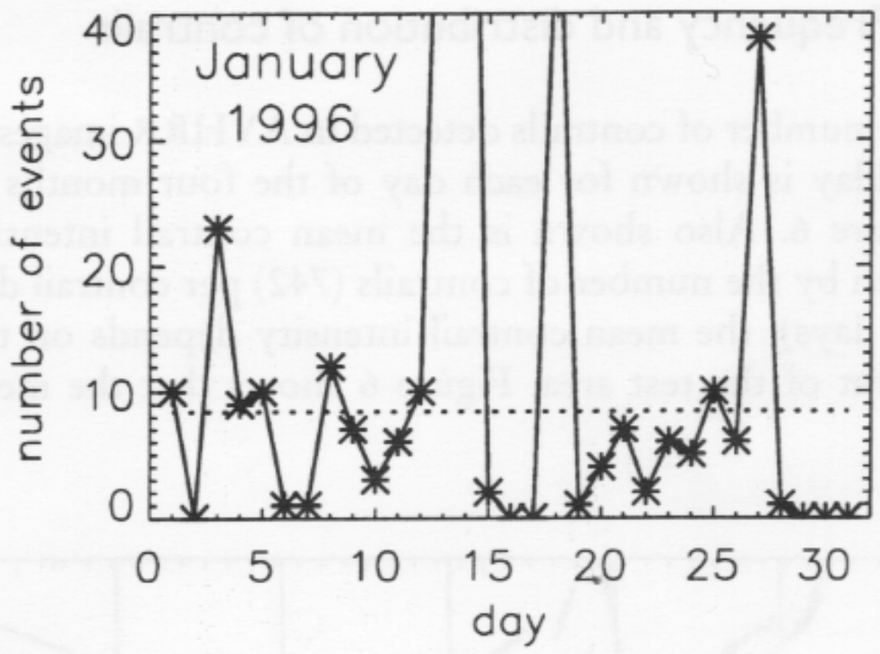

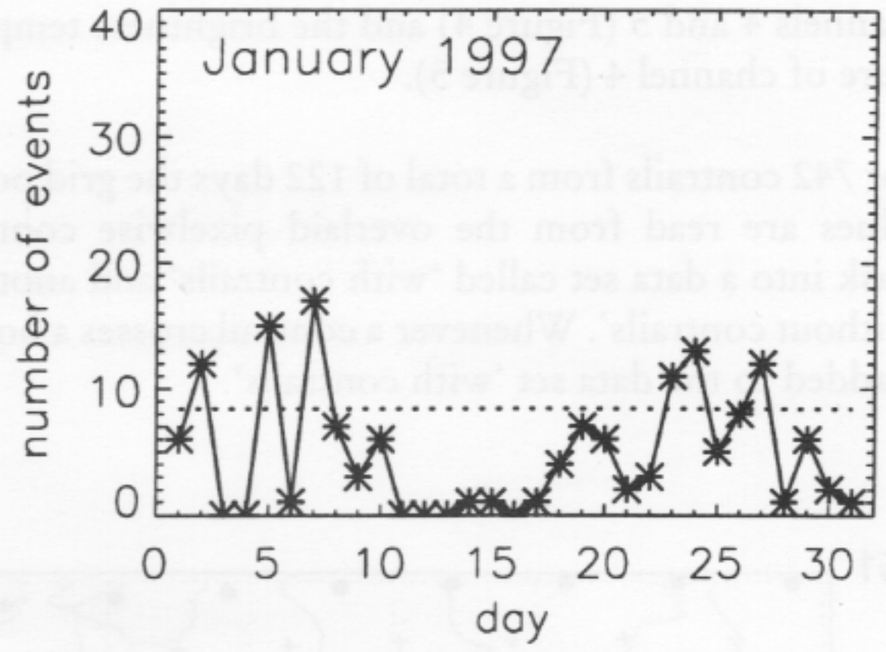

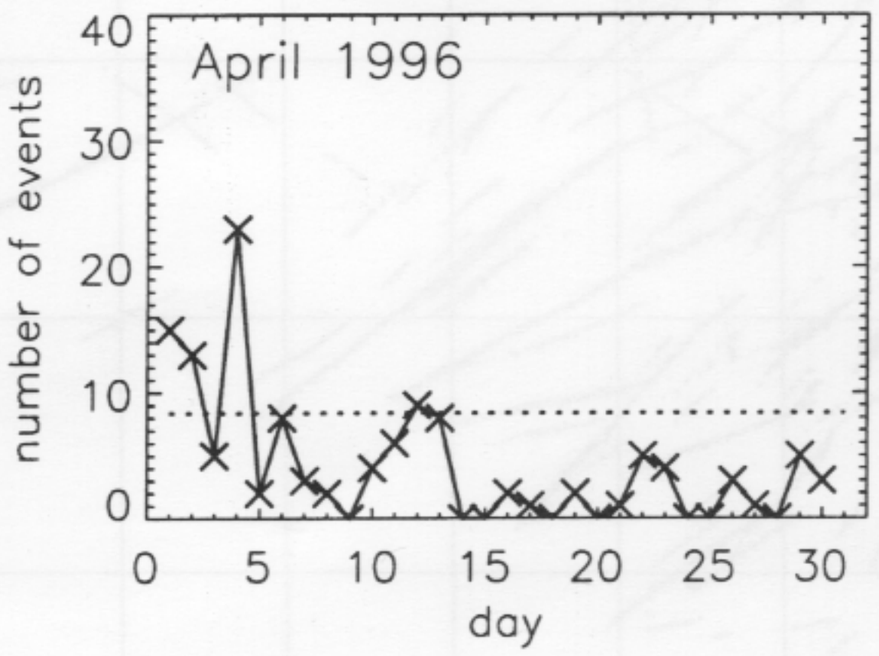

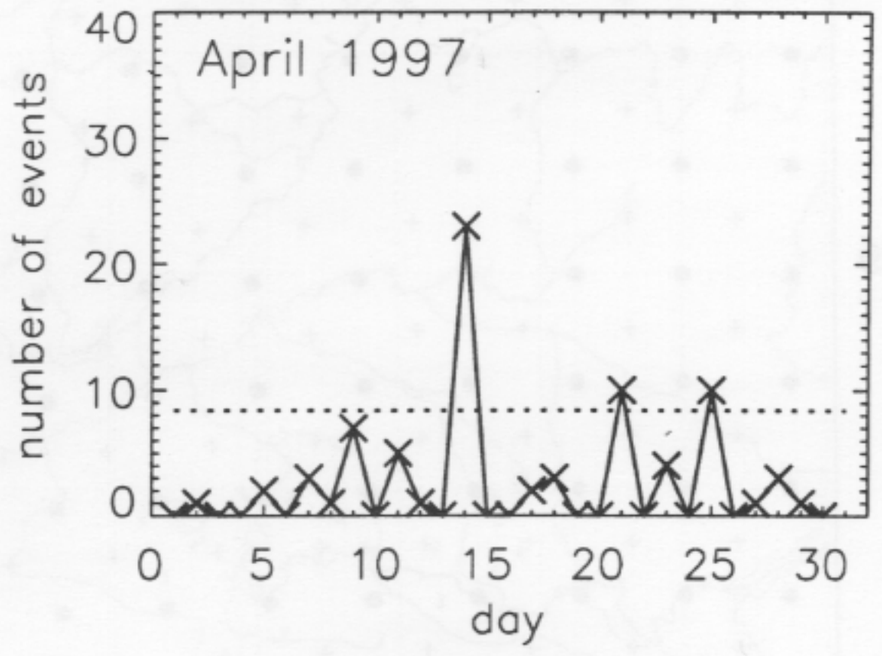

Figure 6. *Number of contrails over Bavaria at midday for January and April in 1996 and 1997.*

value is not the most frequent one and that it is surpassed only on a few days. This suggests that there are special meteorological situations prevailing when many contrails are present.

Seasonal differences are noticeable in 1996. In January there are many more contrails than in April, but it should be kept in mind that the contrail detection method is usually more effective in winter than in spring owing to smaller temperature variance in winter over fog or stratus. In 1997 the seasonal differences are not as pronounced as in 1996. In January 1996 the number of contrails is twice as high as in January 1997; thus the seasonal and annual variability of contrail occurrence have the same order of magnitude. The great variability of the contrails is apparent: on a single day in January 1996 more contrails occurred than during the entire following April. On such single days the additional artificial cloud cover of contrails considerably exceeds the typical value of a 0.5%. On the other hand, this great variability means that the investigation to get significant mean conditions needs to be based on more than the 122 days used here.

In this study we count the contrails without regarding their cloud cover, because it is aimed at inspecting atmospheric regions where contrails are mainly apparent. Nevertheless, the daily geographical distribution of cloud cover due to contrails is determined with an automated algorithm for two years in 666 NOAA-14 passages from March 1995 to February 1997 (Meyer *et al.*, 1998). From these daily data an annual cloud cover of the contrails is estimated to be 0.5%. The seasonal means for winter (December 1995 – February 1996, December 1996 – February 1997) and summer (June – August in 1995 and 1996) are shown in Figures 7 and 8. A maximum of contrail cloud cover is directed from north-west to south-east across Bavaria along the main jet flight routes (overlaid). This pattern is more obvious in winter, while in summer the distribution is more uniform. Over the Alps the contrail detection is not performed owing to the high spatial variability of the surface conditions.

4. Contrails and EM parameters

In this study only those five layers of the EM between 7 and 12 km altitude, where the main air traffic takes place, were considered. Figure 9 shows the mean thermodynamic properties and the standard deviations for all the 742 contrails that were identified. Within contrails some supersaturation relative to ice is dominant just below the tropopause at about 9 km altitude (see Figure 9(*a*)) where there is also slow ascent ($\omega < 0$) as in warm frontal zones (see Figure 9(*b*)). An air parcel at 9

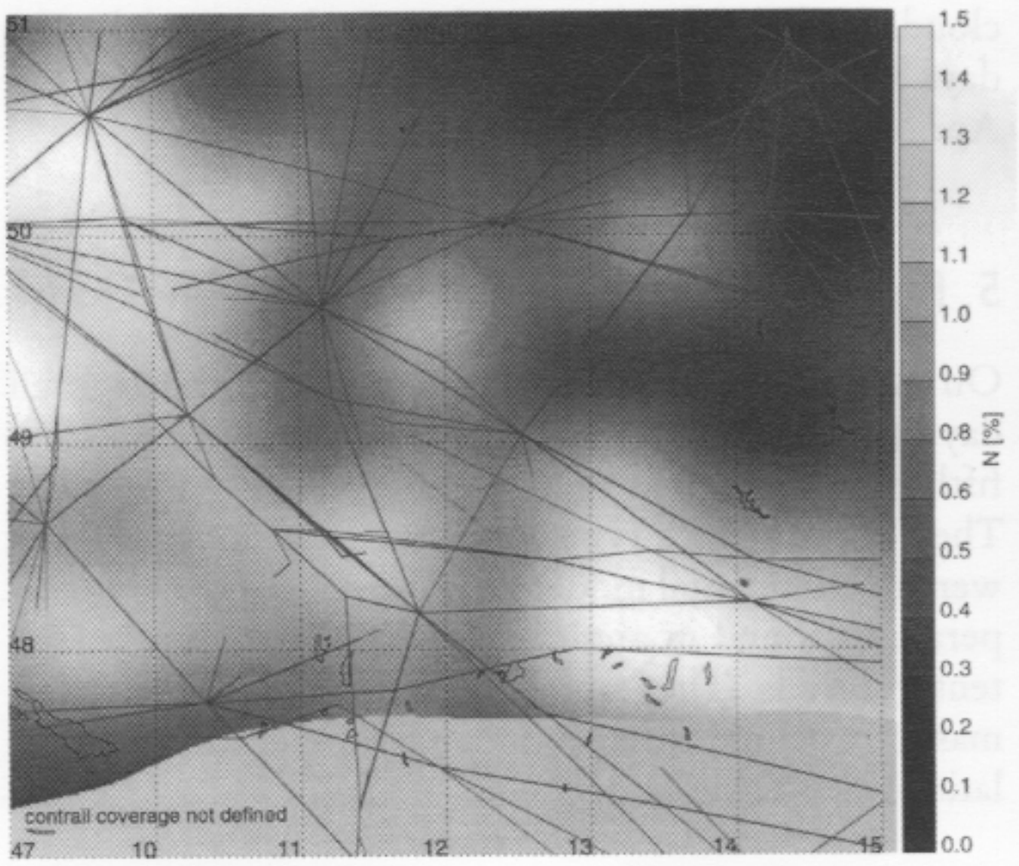

Figure 7. *Additional cloud cover of linear contrails at noon in winter (data from December 1995 to February 1996 and December 1996 to February 1997). The jet flight routes above 20000 ft are overlaid.*

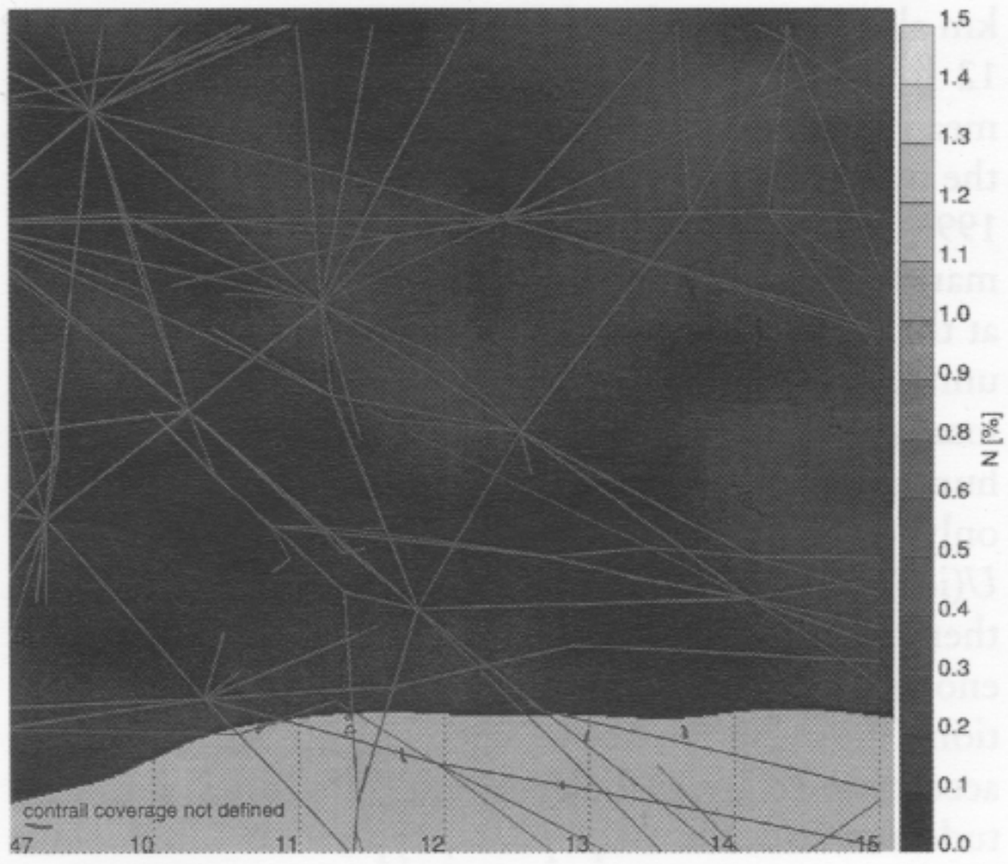

Figure 8. *As Figure 7, but in summer (data from June to August 1996 and 1997).*

(a)

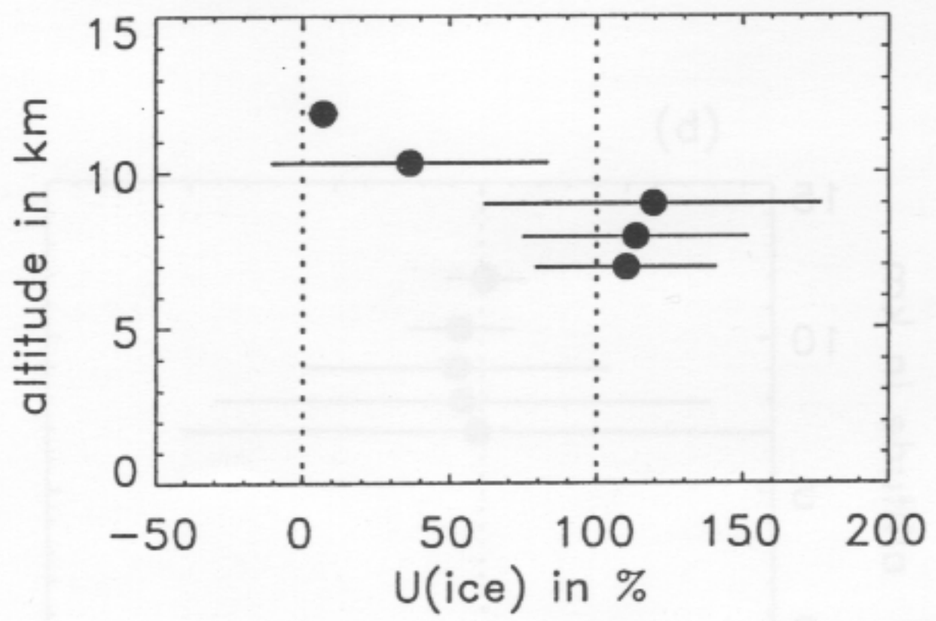

(b)

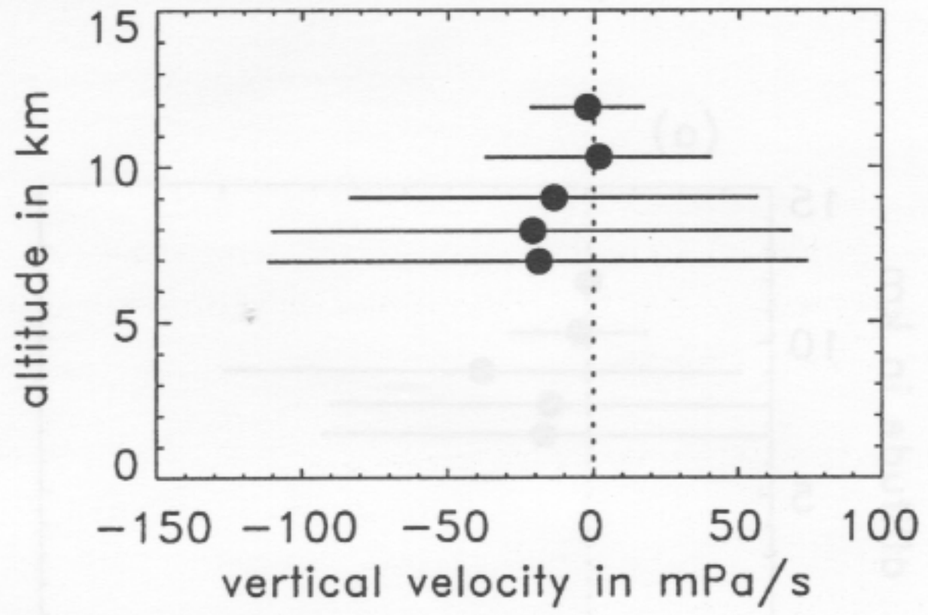

(c)

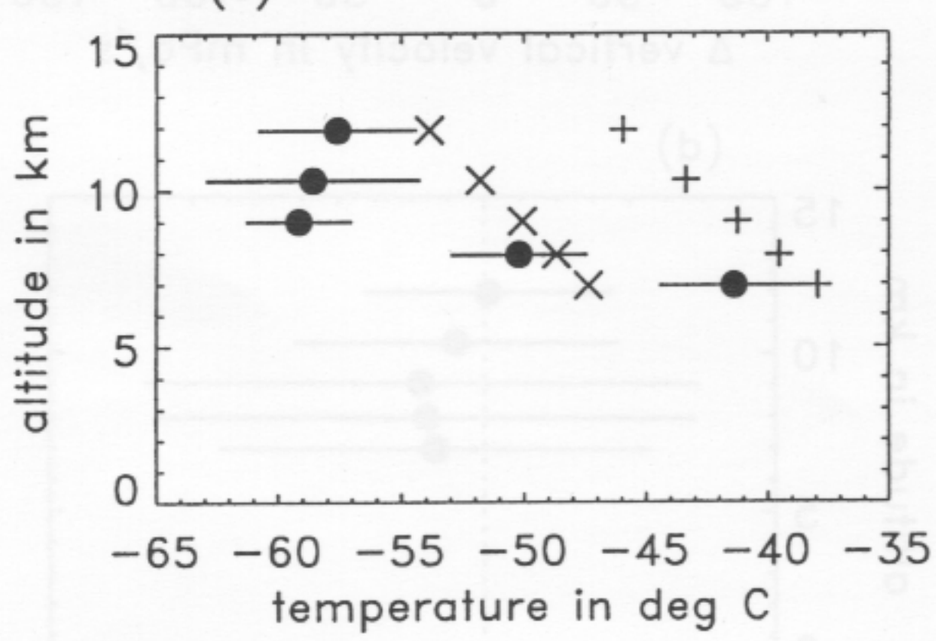

(d)

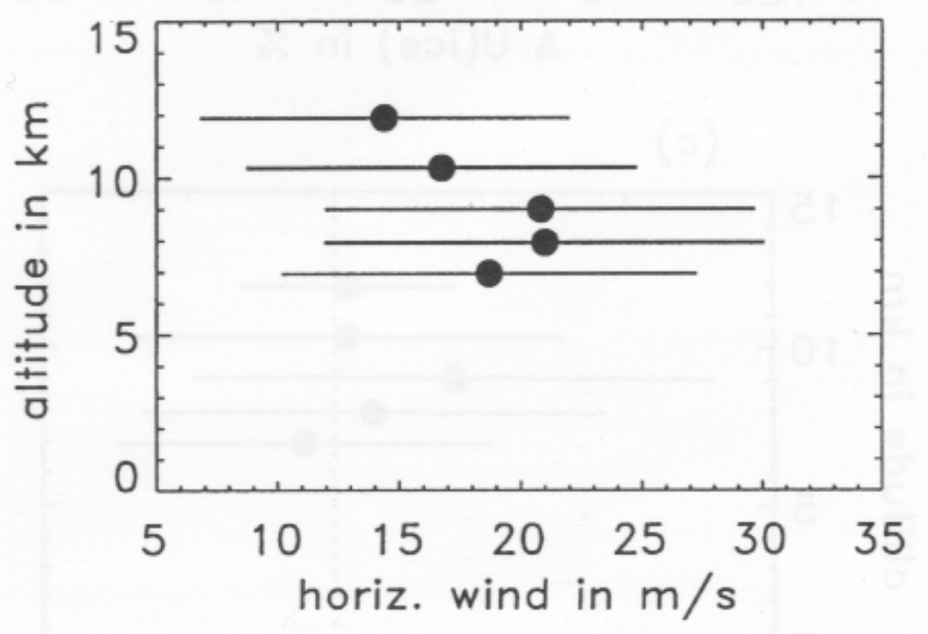

Figure 9. *Mean (dots) and standard deviation (bars) of the thermodynamic parameters for data set 'with contrail' in five EM levels between 7 and 12 km altitude. The relative humidity U related to ice is shown in* (a), *the vertical velocity* ω ($\omega < 0$ *for upward motion) in* (b), *the temperatures in* (c). *Additionally, in* (c) *the probability of contrail occurrence is marked by temperature values in each level: left of the '×' signs the probability is unity, right of the '+' signs it is zero. The mean horizontal wind velocity is shown in* (d).

km altitude is lifted with constant ($\omega = -100$ mPa s^{-1} in 12 h to about 10 km altitude. Figure 9(*c*) shows the mean temperatures and the temperatures according to the modified Appleman–Schmidt criterion (Schumann, 1996). At the warm side in Figure 9(*c*) (right of the '+' mark) the probability of contrail occurrence is zero and at the cold side (left of the '×' marks) the probability is unity. When the temperature profile is between these marks, the contrail occurrence depends on the relative humidity over ice. On average, this situation is met only at 7 km. But there, on average, the humidity U(ice) exceeds 100%, and thus contrails are probable there as well. Above, the atmosphere is always cold enough in winter and spring to support contrail formation. The mean horizontal wind (Figure 9(*d*)) is strong, accompanied by turbulence, and intensifies with altitude towards the tropopause, typical of a baroclinic atmosphere where shear winds cause the contrails to spread more quickly. All these EM parameters have large standard deviations. Therefore, the difference between neighbouring regions with and without contrails is not significant when looking at each parameter separately. Apparently, the atmosphere with contrails is usually more humid and colder and the wind is stronger (Figure 10) than where there are no contrails. The neighbourhood of contrails was cloudy in most cases, often with cirrus clouds at the same level; thus the thermodynamic properties of contrails and cirrus clouds could not be distinguished. Only on 2 of the 122 days were there contrails over Bavaria in January and April in an otherwise cloudfree region.

5 Results of the analysis of weather conditions

On average, contrails are detected on two-thirds of all days (winter, spring) over Bavaria, but only on one-fifth of all days was their number above the average. They occur in each type of air mass, but most of them were in continental moderate polar air, as the cold temperatures found in arctic and polar air support persistent contrails. They appear mainly in a changing air mass (baroclinic zone) and mainly in meridional circulations (see Table 1).

A typical weather situation giving many contrails in Bavaria is a low in north Italy (a moving Genoa-cyclone), where warm moist Mediterranean air is lifted towards the tropopause from a southerly direction. Contrails form at altitudes preceding the formation of cirrus and cirrostratus with the approaching warm front. The relative humidity over ice is crucial at lower levels, but the originally warm Mediterranean air typically has high humidities.

Another weather situation with many contrails in the

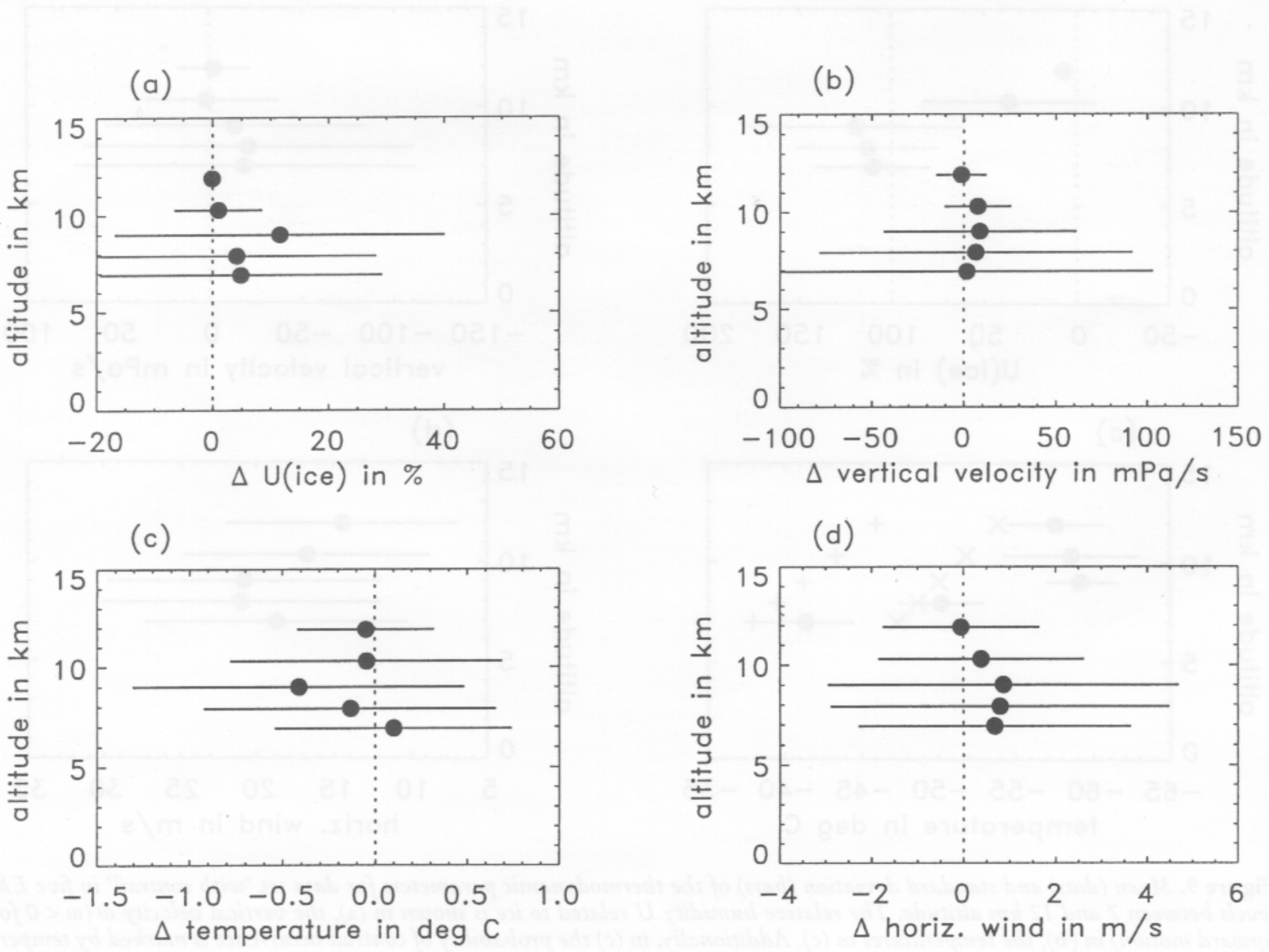

Figure 10. *As Figure 9, but differences between parameters 'with' and 'without' contrails.*

Table 1. *Circulation and contrails in Bavaria for January and April, 1996 and 1997; contrail intensity indicates the number of contrails per contrail-day*

Circulation	Days	Contrail-days	Number of contrails	Contrail intensity
Zonal	4	2	14	7.0
Mixed	40	26	82	3.2
Meridional	78	60	646	10.8
Total	122	88	742	8.4

upper atmosphere is ahead of surface cold fronts within the warm air. Contrails are artificial cirrus clouds and they occur at places where natural cirrus could exist as well. There are two types of cold front, both associated with a typical cloud formation (e.g. given in Kurz, 1993). In a slow-moving cold front there may be a cirrus shield ahead around a thunderstorm. Figure 11 illustrates the model of a slow-moving cold front. The warm conveyor belt across the front is dotted; cold air (C) moves against warm air (W). The cross-section from A to B shows the thunderstorm (Cb) just above the surface cold front within the warm air, and contrails are expected at the position of B ahead of the surface cold front. The turbulent upward motion supplies the upper atmosphere with sufficient moisture that supports contrail formation. Figure 12 shows the model of a fast-running cold front where again convective complexes (Cu) are above the surface front within the warm air, indicating turbulent upward motion. Contrails may form there. Further, they are expected at a second place in a fast-running cold front, namely, within the upper part of the warm conveyor belt far ahead of the cold front.

Figure 13 shows the horizontal wind in 280 hPa at 1200 UTC on 14 January 1996 taken from the EM data in the

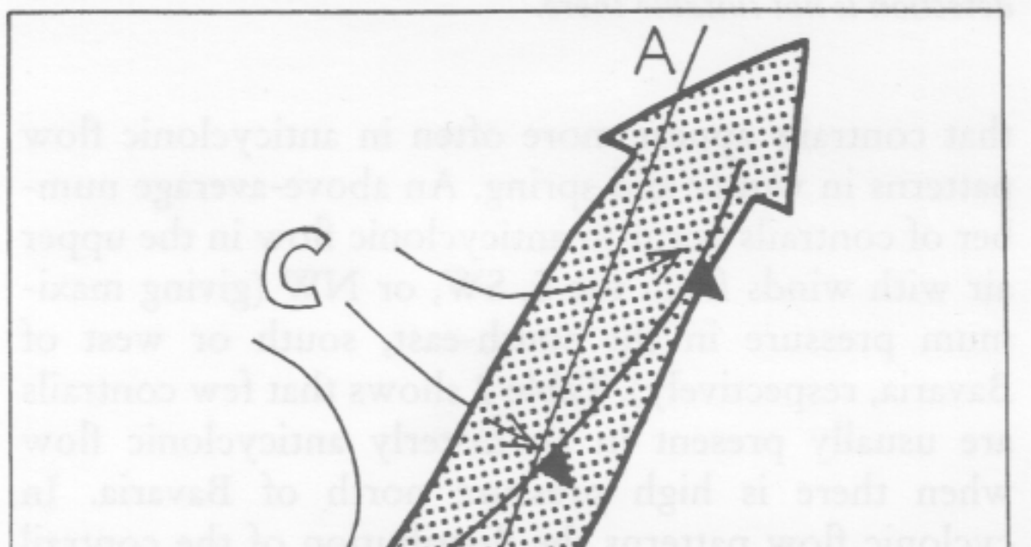

Figure 11. *Schematic diagrams of a slow-moving cold front (after Kurz, 1993). Plan view with dotted warm conveyor belt (top) and vertical cross-section along line AB (bottom). The appearence is similar to a warm front but of course the clouds and rain are arranged post-frontal.*

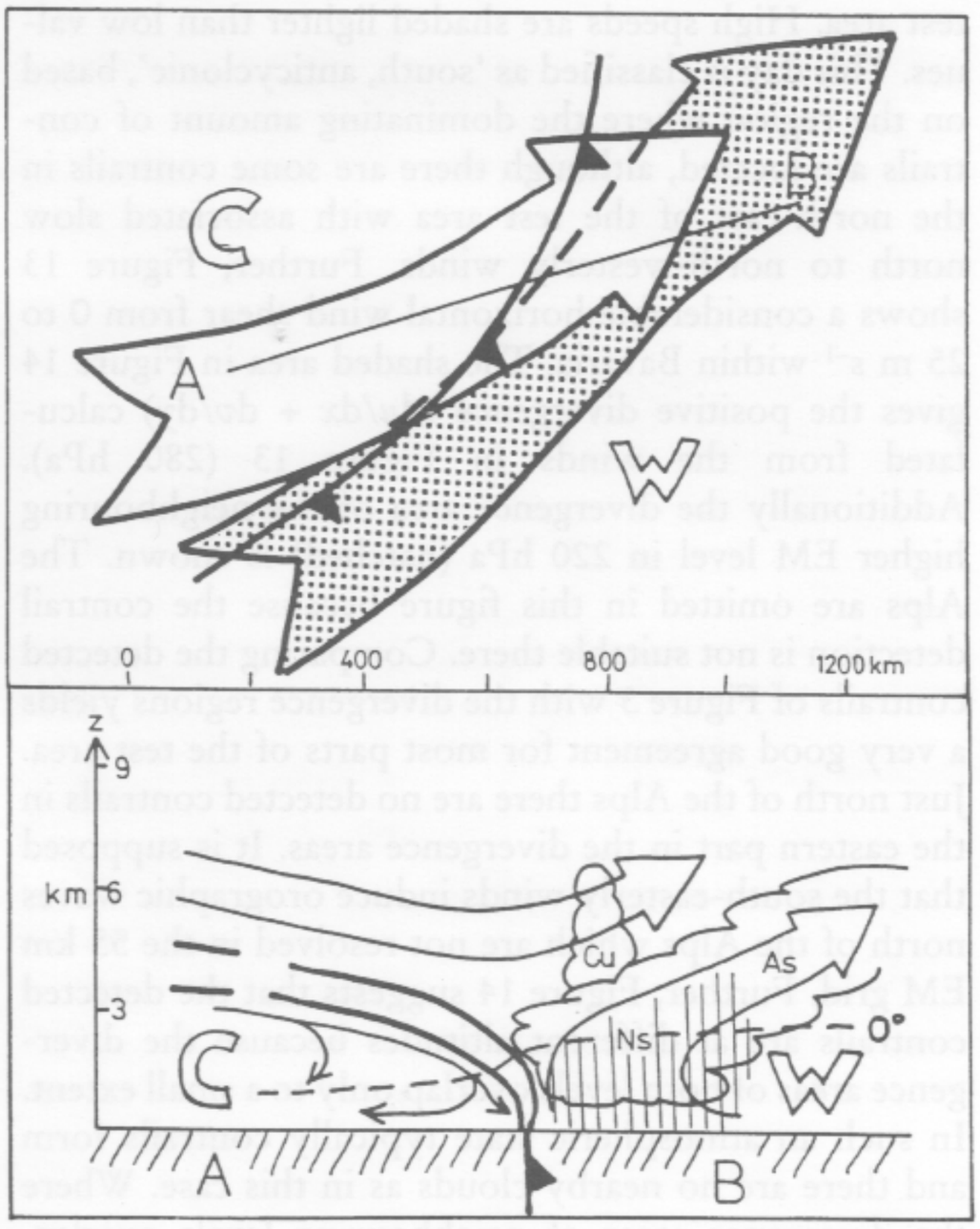

Figure 12. *Schematic diagrams of a fast-running cold front (after Kurz, 1993). Plan view with upper relative motion of dry cold air crossing the surface cold front above the dotted warm conveyor belt (top). The cross-section along line AB (bottom) shows that the warm conveyor belt is inclined ahead of the cold front by the relative dry flow from behind of the front.*

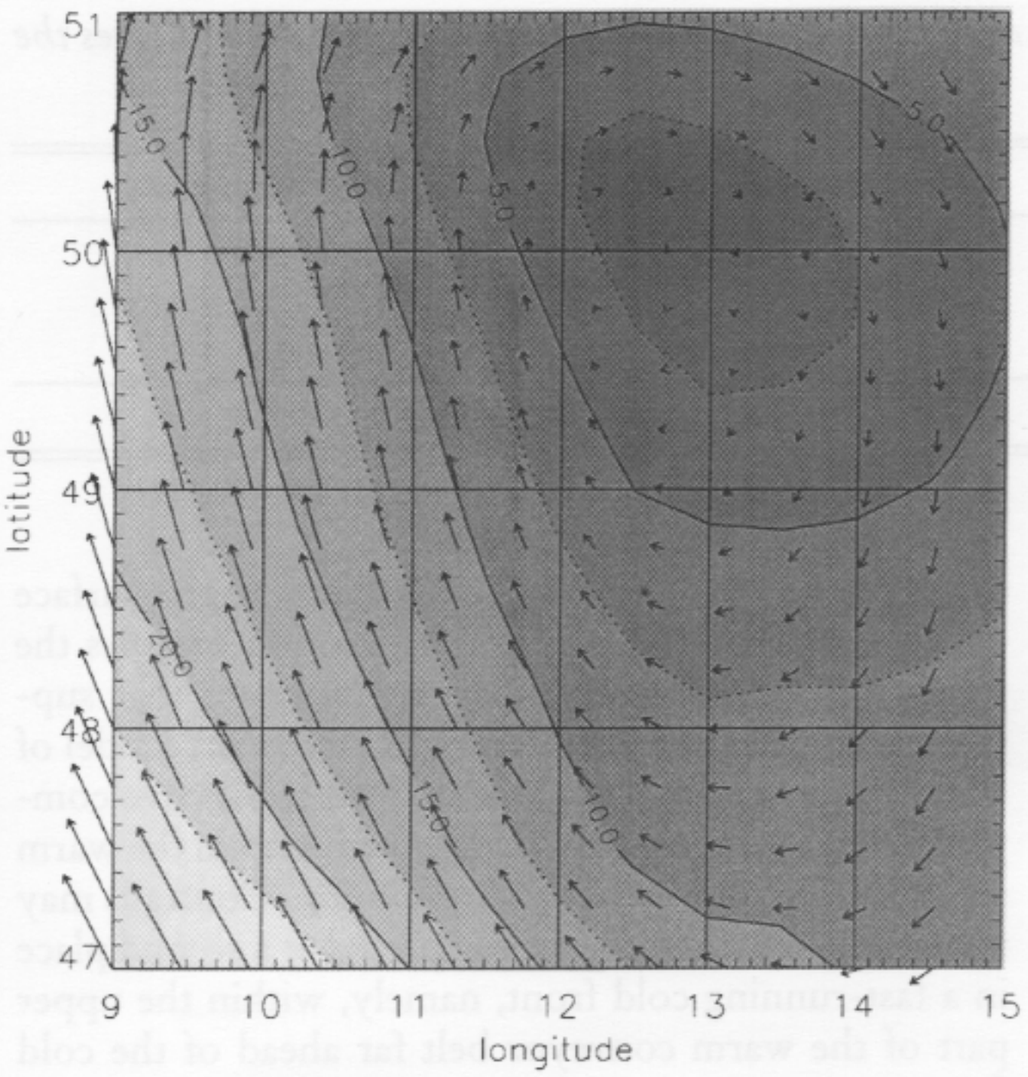

Figure 13. *Horizontal wind in 280 hPa from EM data on 14 January 1996 in Bavaria. The length of the wind arrows is according to the wind velocity which is additionally given by isotachs (m s^{-1}).*

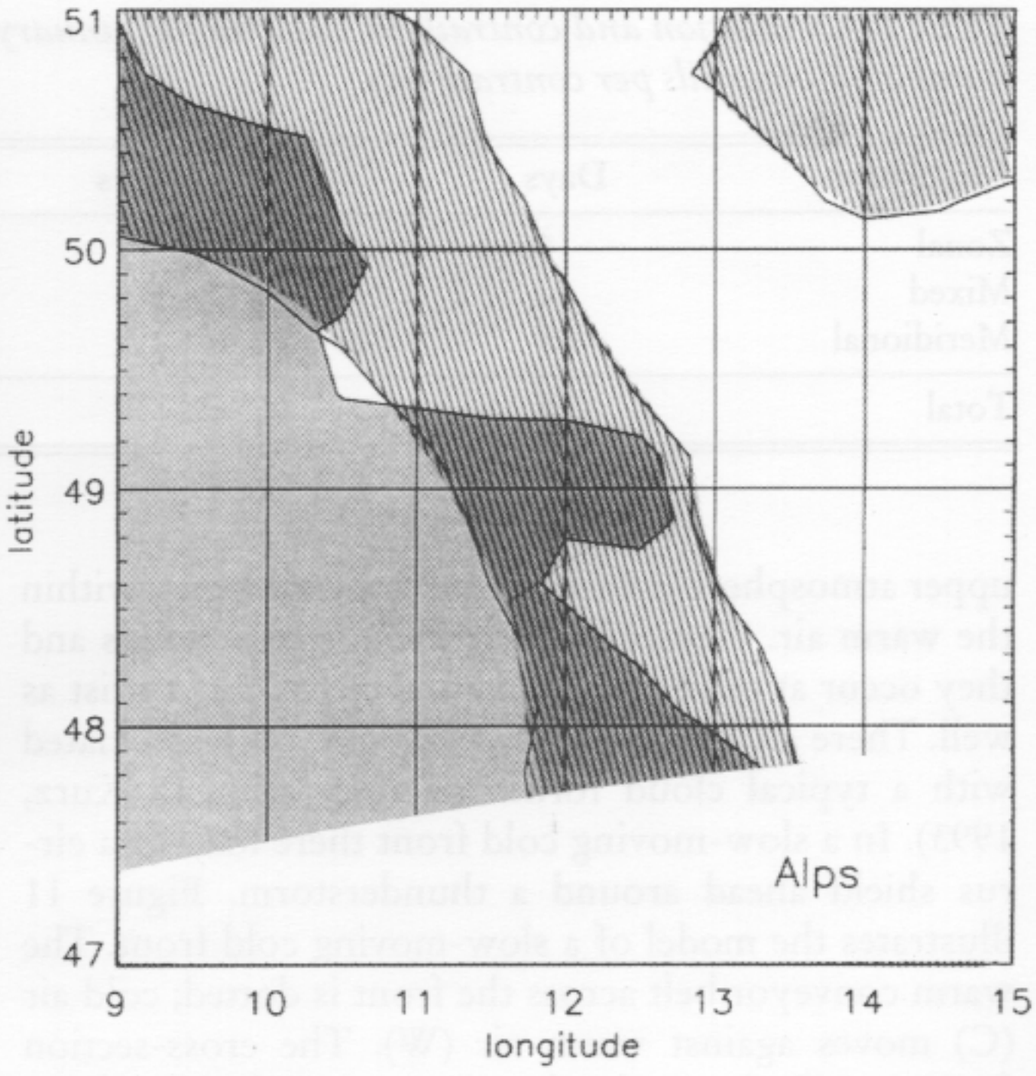

Figure 14. *Divergence on 14 January 1996 at two EM levels: 280 hPa (shaded) and 220 hPa (hatched). The divergence areas correspond to the regions with many contrails (compare with Figure 3). The Alps are omitted because the contrail detection is not suitable there.*

test area. High speeds are shaded lighter than low values. This day is classified as 'south, anticyclonic', based on the region where the dominating amount of contrails are located, although there are some contrails in the north-east of the test area with associated slow north to north-westerly winds. Further, Figure 13 shows a considerable horizontal wind shear from 0 to 25 m s^{-1} within Bavaria. The shaded area in Figure 14 gives the positive divergence ($du/dx + dv/dy$) calculated from the winds in Figure 13 (280 hPa). Additionally the divergence area of the neighbouring higher EM level in 220 hPa (hatched) is shown. The Alps are omitted in this figure because the contrail detection is not suitable there. Comparing the detected contrails of Figure 3 with the divergence regions yields a very good agreement for most parts of the test area. Just north of the Alps there are no detected contrails in the eastern part in the divergence areas. It is supposed that the south-easterly winds induce orographic waves north of the Alps which are not resolved in the 55 km EM grid. Further, Figure 14 suggests that the detected contrails are at different altitudes because the divergence areas of both levels overlap only to a small extent. In such an atmospheric state typically contrails form and there are no nearby clouds as in this case. Where the divergence areas of neighbouring levels overlap, clouds are expected, and indeed there is thin cirrus seen in the satellite image (not shown).

As with this example, each studied day is categorised according to the wind direction and the curvature of the flow. The analysis of weather types (Table 2) shows that contrails appear more often in anticyclonic flow patterns in winter and spring. An above-average number of contrails occur in anticyclonic flow in the upper air with winds from the S, SW, or NW (giving maximum pressure in the south-east, south or west of Bavaria, respectively). Table 2 shows that few contrails are usually present in an easterly anticyclonic flow when there is high pressure north of Bavaria. In cyclonic flow patterns the distribution of the contrail intensity, defined as contrails per contrail-day, is more uniform, peaking at SE weather types (moving Genoa-cyclone). Although many contrails occur in upper cyclonic SW winds, the corresponding intensity is rather small. In cyclonic circulations the contrail intensity over Bavaria is highest with SW winds followed by NW winds. The contrails mainly occur near local wind maxima of jet streams just below the tropopause.

In conclusion, two main meteorological situations are found which have many persistent contrails:

(a) slow ascent of upper air far ahead of a surface warm front often near jet streams, and
(b) in more convective and turbulent regions with strong winds ahead of a surface cold front.

Another situation which is not as pronounced as the other two is in regions where the geopotential has a strong curvature (e.g. in the axis of a high-pressure ridge; the ridge gets smaller as a front approaches and the curvature at the ridge axis increases and thus the wind shear increases). A common feature in these situ-

Table 2. *Circulation (based on upper-wind direction and curvature) and contrails in Bavaria for January and April, 1996 and 1997; maximum values are in bold*

Circulation	Days	Contrail-days	No. of contrails	Contrail intensity
Anticyclonic				
N	12	10	26	2.6
NE	6	4	11	2.8
E	5	1	2	2.0
SE	1	1	2	2.0
S	5	4	93	**23.3**
SW	10	9	**139**	15.9
W	7	5	23	4.6
NW	**16**	**11**	111	10.1
Total anticyclonic	62	45	407	9.0
Cyclonic				
N	5	1	9	9.0
NE	3	2	12	6.0
E	3	3	26	8.7
SE	4	3	37	**12.3**
S	5	5	42	8.4
SW	**22**	**19**	**126**	6.6
W	6	3	12	4.0
NW	12	7	71	10.1
Total cyclonic	60	43	355	7.8
Total	122	88	742	8.4

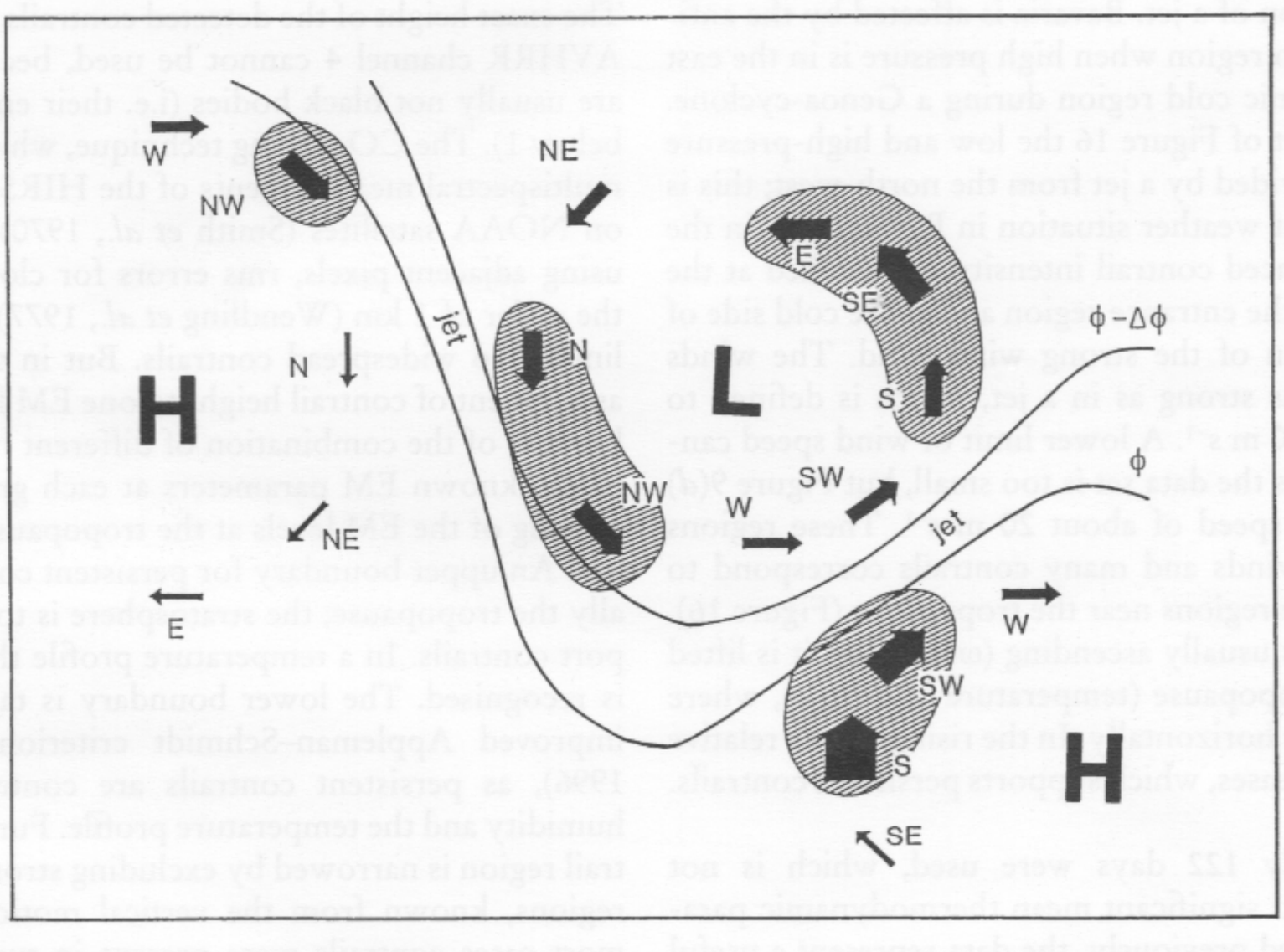

Figure 15. *Conceptual scheme of low and high pressure in a meridional flow with regions of enhanced occurrence of contrails (hatched) in the upper troposphere in mid-latitudes with a northwesterly and southwesterly strong wind band; thickness of wind arrows is proportional to contrail intensity given in Table 2.*

ations is a baroclinic atmosphere near the tropopause, where the contrails spread in divergent zones.

These findings lead to a conceptual model for regions with many contrails. Figure 16 shows in the right part the upper atmosphere with minimum (L) and maximum (H) pressure in a meridional circulation divided by a jet stream from the south-west, the most frequent situation in Bavaria. The arrows give the wind direction, but their thickness is proportional to the contrail intensities given in Table 2. There are two regions (hatched) where the contrail intensity is above average:

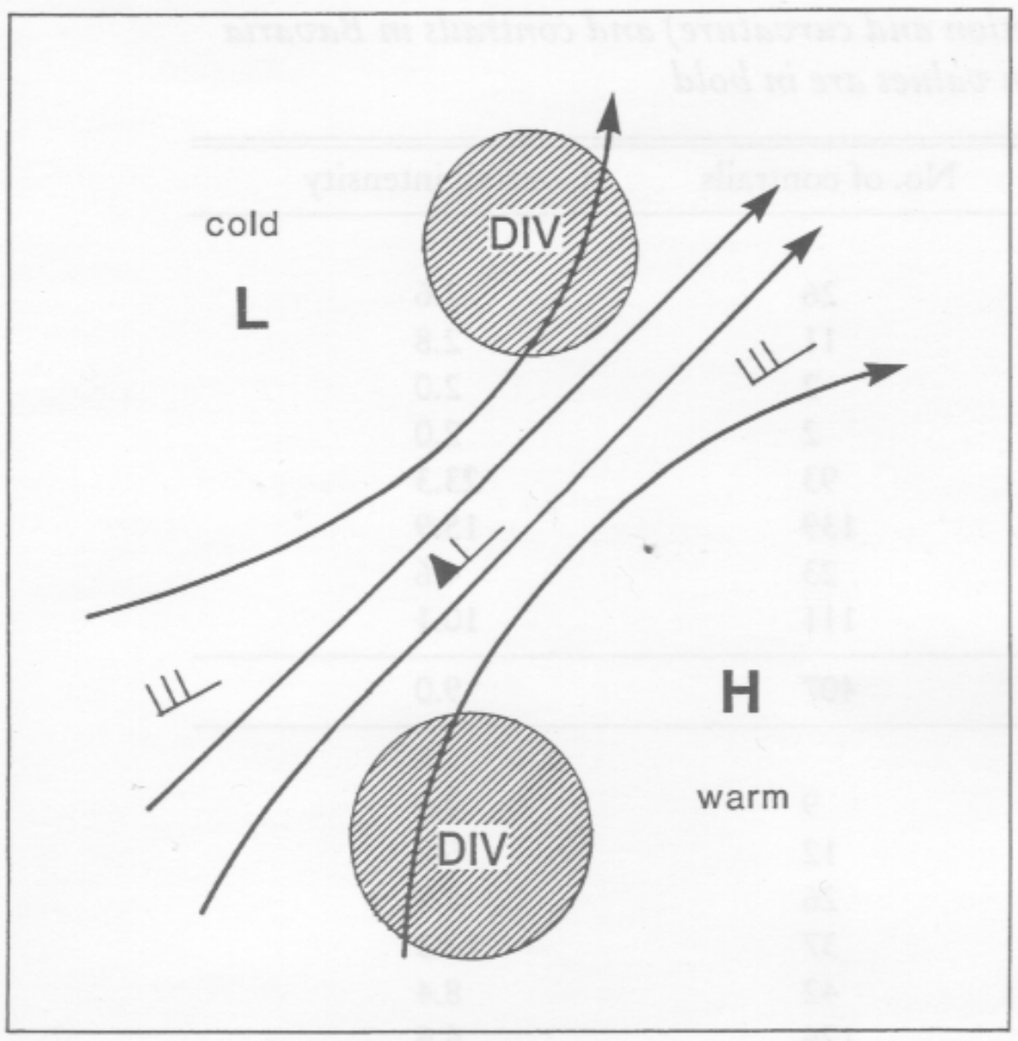

Figure 16. *Divergence regions in a strong wind pattern (after Bluestein, 1992).*

one is in the warm entrance region and the other in the cold exit region of a jet. Bavaria is affected by the anticyclonic warm region when high pressure is in the east and the cyclonic cold region during a Genoa-cyclone. In the left part of Figure 16 the low and high-pressure system are divided by a jet from the north-west; this is also a frequent weather situation in Bavaria. Again the areas of enhanced contrail intensity are hatched at the warm side of the entrance region and at the cold side of the exit region of the strong wind band. The winds need not be as strong as in a jet, which is defined to have at least 30 m s^{-1}. A lower limit of wind speed cannot be given as the data set is too small, but Figure 9(*d*) gives a mean speed of about 20 m s^{-1}. These regions with strong winds and many contrails correspond to the divergence regions near the tropopause (Figure 16). Here the air is usually ascending ($\omega < 0$) and it is lifted against the tropopause (temperature inversion), where the air spreads horizontally. In the rising air the relative humidity increases, which supports persistent contrails.

Although only 122 days were used, which is not enough to find significant mean thermodynamic parameters as stated previously, the data represent a useful source to demonstrate the correspondence between contrail occurrence and divergence regions in the upper atmosphere.

6. Conclusion and discussion

This study aims to determine the atmospheric conditions that favour persistent contrails. It should be useful for both contrail forecasting and estimates of cloud cover increase within an increasing air traffic scenario.

In a test area in central Europe, contrails are detected in AVHRR measurements with 1 km resolution. Fog and stratus, which occur most often in winter, improve the detectability of contrails. On the whole, the automated multispectral contrail detection algorithm proves to be an appropriate tool for monitoring daily linear contrails. Only on a few occasions are small clouds in line structures (e.g. cumulus streets or line-shaped cloud shadows) misinterpreted as contrails.

The EM gridpoints are read manually from an overlaid contrail mask whenever a contrail crosses the gridpoint box. Mean values of all contrail-contaminated gridpoints show a large standard variation, the contrail grid points have higher humidity, lower temperatures and higher wind speeds than neighbouring gridpoints, but the difference between contrail-contaminated and contrail-free neighbouring gridpoints is not found to be statistically significant. With regard to the results of the weather analysis of contrail days it is assumed that first selecting weather conditions and then calculating mean values is a better way to produce typical mean values of thermodynamic parameters for contrails.

The exact height of the detected contrails is not known. AVHRR channel 4 cannot be used, because contrails are usually not black bodies (i.e. their emissivity is far below 1). The CO_2 slicing technique, which is based on multispectral measurements of the HIRS-2 instrument on NOAA satellites (Smith *et al.*, 1970) yields, when using adjacent pixels, rms errors for cloud heights of the order of 1 km (Wendling *et al.*, 1977); this result is limited to widespread contrails. But in this study the assignment of contrail height to one EM level is unique because of the combination of different height profiles of the known EM parameters at each grid point. The spacing of the EM levels at the tropopause is about 1.1 km. An upper boundary for persistent contrails is usually the tropopause; the stratosphere is too dry to support contrails. In a temperature profile the tropopause is recognised. The lower boundary is taken from the improved Appleman–Schmidt criterion (Schumann, 1996), as persistent contrails are controlled by the humidity and the temperature profile. Further, the contrail region is narrowed by excluding strong subsidence regions, known from the vertical motion profile. In most cases contrails were present in turbulent zones around the wind maximum where vertical and horizontal shear winds are present.

The relation of contrail occurrence and divergent regions is very useful for a forecast of contrails (e.g. in experimental flight campaigns). Usually, horizontal winds are forecast very well in contrast to vertical winds. From the gradient of the horizontal wind and its curvature the divergence regions are determined by an isotach analysis. In a divergent flow persistent contrails

broaden, which supports the detection of contrails in AVHRR measurements.

Thus, persistent contrail regions near the tropopause in mid-latitudes and the corresponding dynamic meteorological conditions of a baroclinic atmosphere are obviously related to divergence regions where upward motion dominates (Wendling *et al.*, 1997). This has to be proved in a larger area than Bavaria to exclude local effects, but it is assumed that the upper atmosphere is not affected by them very much.

Acknowledgement

We wish to thank Dr H. Mannstein for many rich discussions and his assistance in data handling. This work was funded by the Bundesministerium für Bildung und Forschung (BMFT) under contract no. AP 1311 of the program 'Schadstoffe in der Luftfahrt', by the Bavarian climate research programme BayFORKLIM under contract no. H3, and by the Commission of the European Communities (CEC) under contract ENV4-CT95-0157. The fruitful cooperation with the DWD is gratefully acknowledged.

References

Appleman, H. S. (1953). The formation of exhaust condensation trails by jet aircraft. *Bull. Am. Meterol. Soc.*, **34:** 14–20.

Bakan, S., Betancor, M., Gayler, V. & Grassl, H., (1994). Contrail frequency over Europe from NOAA-satellite images. *Ann. Geophys.*, **12:** 962–968.

Bluestein, H. (1992). *Synoptic-dynamic Meteorology in Midlatitudes*, Vol. II: *Observation and Theory of Weather Systems.* Oxford University Press, 594 pp.

Engelstad, M., Senupta, S. K., Lee, T. & Welch, R. M. (1992). Automated detection of jet contrails using the AVHRR split window. *Int. J. Remote Sensing,* **13:** 1391–1412.

Freudenthaler, V., Homburg, F. & Jaeger, H., (1995). Contrail observations by ground-based scanning lidar: cross-sectional growth. *Geoph. Res. Letters,* **22:** 3501–3504.

Gerstengarbe, F.-W. & Werner, P. C., (1993). Katalog der Grosswetterlagen Europas nach Paul Hess und Helmuth Brezowski 1881–1992. *Berichte des DWD,* **113**, Deutscher Wetterdienst, 249 pp.

Kärcher, B., Peter, T., Biermann, U. M. & Schumann, U. (1996). The initial composition of jet condensation trails. *J. Atmos. Sci.*, **53:** 3066–3083.

Knollenberg, R. G. (1972). Measurements of the growth of the ice budget in a persisting contrail. *J. Atmos. Sci.*, **29:** 1367–1374.

Kurz, M. (1990). *Synoptische Meteorologie*. Deutscher Wetterdienst, 197 pp.

Liou, K. N. (1986). Influence of cirrus clouds on weather and climate processes: a global perspective. *Mon. Wea. Rev.*, **114:** 1167–1198.

Mannstein, H., Meyer, R. & Wendling, P. (1998). Operational detection of contrails from NOAA-AVHRR-data, *Int. J. Remote Sensing*, in press.

Meyer, R., Mannstein, H. & Wendling, P. (1998). Contrail coverage of Western Europe derived from 2 years of NOAA-AVHRR-data, *Proc. of the 9th AMS Conference on Satellite Meteorology and Oceanography, Paris, 25–29 May 1998,* 266–269.

Peppler, W. (1930). Wolkenbildungen durch Flugzeuge. *Ztschr. f. angew. Meteor.*, **47:** 35–46.

Ponater, M., Brinkop, S., Sausen, R. & Schumann, U. (1996). Simulating the global atmospheric response to aircraft water vapour emissions and contrails: a first approach using a GCM. *Ann. Geophys.*, **14:** 941–960.

Sausen, R., Gierens, K., Ponater, M. & Schumann, U. (1998). A diagnostic study of the global coverage by contrails, part I: present day climate. *Theor. Appl. Clim.*, in press.

Schumann, U. (1996). On conditions for contrail formation from aircraft exhausts. *Meteorol. Z.*, **N. F. 5:** 4–23.

Smith, W. L., Woolf, H., M. & Jacob, W. J. (1970). A regression method for obtaining real-time temperature and geopotential height profiles from satellite spectrometer measurements and its application to Nimbus 3 SIRS observations. *Mon. Wea. Rev.*, **98:** 604–611.

Sonntag, D. (1994). Advancements in the field of hygrometry. *Meteorol. Z.*, **N. F. 3:** 51–66.

Spinhirne, J. D., Hart, W. D. & Duda, D. P. (1998). Evolution of the morphology and microphysics of contrail cirrus from airborne remote sensing. *Geophys. Res. Lett.*, **25:** 1153–1156.

Strauss, B., Meerkoetter, R., Wissinger, B., Wendling, P. & Hess, M. (1997). On the regional climatic impact of contrails – microphysical and radiative properties of contrails and natural cirrus clouds. *Ann. Geophys.*, **15:** 1457–1467.

Travis, D. J. (1996). Variations in contrail morphology and relationships to atmospheric conditions. *J. Wea. Mod.*, **28:** 50–59.

Travis, D. J., Carleton, A. M. & Changnon, S. A. (1997). An empirical model to predict widespread occurances of contrails. *J. Appl. Meteorol.*, **36:** 1211–1220.

Wendling, P., Buell, R., Kästner, M., Mannstein, H., Meyer, R., Schröder, F. & Strauss, B. (1997). *Bestimmung der Kondensstreifenbewoelkung in Sueddeutschland mit Hilfe von Satellitenmessungen.* Deutsche Forschungsanstalt fuer Luft- und Raumfahrt e.V., DLR, Institut fuer Physik der Atmosphaere, 70 pp.